Fission yeast MOZART1/Mzt1 is an essential γ-tubulin complex component required for complex recruitment to the microtubule organizing center, but not its assembly

Hirohisa Masuda[a], Risa Mori[a], Masashi Yukawa[a,b], and Takashi Toda[a]
[a]Laboratory of Cell Regulation, Cancer Research UK, London Research Institute, Lincoln's Inn Fields Laboratories, London WC2A 3LY, United Kingdom; [b]Department of Molecular Biotechnology, Graduate School of Advanced Sciences of Matter, Hiroshima University, Higashi-Hiroshima 739-8530, Japan

ABSTRACT **γ-Tubulin plays a universal role in microtubule nucleation from microtubule organizing centers (MTOCs) such as the animal centrosome and fungal spindle pole body (SPB). γ-Tubulin functions as a multiprotein complex called the γ-tubulin complex (γ-TuC), consisting of GCP1–6 (GCP1 is γ-tubulin). In fungi and flies, it has been shown that GCP1–3 are core components, as they are indispensable for γ-TuC complex assembly and cell division, whereas the other three GCPs are not. Recently a novel conserved component, MOZART1, was identified in humans and plants, but its precise functions remain to be determined. In this paper, we characterize the fission yeast homologue Mzt1, showing that it is essential for cell viability. Mzt1 is present in approximately equal stoichiometry with Alp4/GCP2 and localizes to all the MTOCs, including the SPB and interphase and equatorial MTOCs. Temperature-sensitive *mzt1* mutants display varying degrees of compromised microtubule organization, exhibiting multiple defects during both interphase and mitosis. Mzt1 is required for γ-TuC recruitment, but not sufficient to localize to the SPB, which depends on γ-TuC integrity. Intriguingly, the core γ-TuC assembles in the absence of Mzt1. Mzt1 therefore plays a unique role within the γ-TuC components in attachment of this complex to the major MTOC site.**

Monitoring Editor
Yixian Zheng
Carnegie Institution

Received: May 3, 2013
Revised: Jul 5, 2013
Accepted: Jul 11, 2013

INTRODUCTION

Microtubules are noncovalent cytoskeletal polymers composed of α- and β-tubulin heterodimers. These heterodimers assemble into linear protofilaments in a GTP-dependent manner, and 13 protofilaments in turn associate laterally to form a 24-nm-wide hollow cylinder. The longitudinal orientation and distinct biophysical properties of α- and β-tubulins give rise to an intrinsic polarity of microtubules, with β-tubulin facing the fast-growing yet dynamic plus end and α-tubulin the less dynamic minus end (Desai and Mitchison, 1997; Nogales, 2000; Jiang and Akhmanova, 2011). The microtubule cytoskeleton plays a myriad of roles inside the cell, in a variety of physiological processes, including cell motility and polarity, cell signaling, organelle positioning, and chromosome segregation. This functional diversification mirrors different microtubule morphologies in various cell types, such as neurons, cilia, and flagella. Even in a single dividing cell, microtubules undergo dynamic structural alterations (e.g., interphase microtubules and bipolar mitotic spindles) in a spatiotemporal manner during the cell cycle.

The key event in microtubule assembly is an initial nucleation. Unlike under certain in vitro situations, in vivo microtubules nucleate from specific sites called the microtubule organizing centers (MTOCs; Pickett-Heaps, 1969; Brinkley, 1985; Luders and Stearns, 2007), where the microtubule minus end is embedded. The MTOC includes the animal centrosome (Boveri, 2008) and the fungi equivalent, the spindle pole body (SPB). Furthermore, in line with the

This article was published online ahead of print in MBoC in Press (http://www.molbiolcell.org/cgi/doi/10.1091/mbc.E13-05-0235) on July 24, 2013.

Address correspondence to: Takashi Toda (takashi.toda@cancer.org.uk).

Abbreviations used: clonNAT, nourseothricin-dihydrogen sulfate; eMTOC, equatorial microtubule organizing center; γ-TuC, γ-tubulin complex; γ-TuRC, γ-tubulin ring complex; γ-TuSC, γ-tubulin small complex; GBP, GFP-binding protein; GRIP, γ-tubulin ring complex protein; iMTOC, interphase microtubule organizing center; MT, microtubule; MTOC, microtubule organizing center; PIC, protease inhibitor cocktail; SPB, spindle pole body; TBZ, thiabendazole; ts, temperature sensitive; WCE, whole-cell extract.

organizational diversities of microtubules, there are numerous other MTOCs besides the centrosome and SPB within cells, among them the basal body for axoneme microtubules, the chromosome for mitotic spindles, and the cell cortex for cortical microtubules (Meng *et al.*, 2008; Mishra *et al.*, 2010; Li *et al.*, 2012). Plant cells do not contain a centrosome equivalent but instead nucleate microtubules from acentrosomal MTOCs, including discrete sites on microtubules and the cell cortex (Murata *et al.*, 2005; Ehrhardt and Shaw, 2006). Despite these structural and spatial variations, most if not all of the microtubules emanate from a universal nucleator called the γ-tubulin complex (γ-TuC; Job *et al.*, 2003; Wiese and Zheng, 2006; Luders and Stearns, 2007).

γ-Tubulin is highly conserved across eukaryotes as a ubiquitous component of the centrosome and SPB (Oakley and Oakley, 1989; Oakley *et al.*, 1990; Horio *et al.*, 1991; Stearns *et al.*, 1991; Stearns and Kirschner, 1994; Zheng *et al.*, 1991; Joshi *et al.*, 1992; Moritz *et al.*, 1995; Sobel and Snyder, 1995; Marschall *et al.*, 1996; Spang *et al.*, 1996). γ-Tubulin does not function on its own, but instead in vivo, it is composed of a large, open, ring structure (~2 MDa and ~32S) via formation of a multiprotein complex with several other nontubulin proteins (referred to as the γ-tubulin ring complex or γ-TuRC; Zheng *et al.*, 1995). These nontubulin complex components are generically designated GCP2–6 (GCP1 is γ-tubulin; Knop *et al.*, 1997; Martin *et al.*, 1998; Murphy *et al.*, 1998; Tassin *et al.*, 1998; Fava *et al.*, 1999; Gunawardane *et al.*, 2000b). Unlike most other eukaryotes, budding yeast contains only three GCPs that mostly form a smaller complex ~300 kDa and 11.3S in size: Tub4/GCP1, Spc97/GCP2, and Spc98/GCP3 (Geissler *et al.*, 1996; Spang *et al.*, 1996; Knop *et al.*, 1997), in a molecular ratio of 2:1:1, respectively (Knop *et al.*, 1997; Vinh *et al.*, 2002). Interestingly, in higher eukaryotes, under high-salt conditions the γ-TuC sedimented with a similar small size (~280 kDa and ~10S) that consists solely of GCP1, GCP2, and GCP3 (referred to as the γ-tubulin small complex or γ-TuSC; Moritz *et al.*, 1998; Oegema *et al.*, 1999; Gunawardane *et al.*, 2000b; Zhang *et al.*, 2000). It was further shown that multiple γ-TuSCs were associated with GCP4, GCP5, and GCP6, which formed γ-TuRCs that possessed more potent microtubule nucleation activity than γ-TuSCs alone (Oegema *et al.*, 1999). In this study, we generally refer to the γ-tubulin complex as the γ-TuC, unless its composition and size are deliberately distinguished as TuSC or TuRC.

Amino acid sequence comparisons of GCP2-6 showed that these proteins share two conserved regions in their C-terminal parts, called GRIP (γ-tubulin ring complex protein) motifs/domains 1 and 2 (Gunawardane *et al.*, 2000a; Teixido-Travesa *et al.*, 2012). The precise molecular function of the GRIP domains has remained enigmatic for some time; however, it has recently become clear that these two domains form virtually identical conformations responsible for direct binding to γ-tubulin (Guillet *et al.*, 2011). This notion has provoked novel insights into the γ-TuRC architecture and the molecular mechanism controlling microtubule nucleation. The previously proposed model in which GCP4, GCP5, and GCP6 were posited to have a capping role at the base of the γ-TuRC distal to γ-tubulin (Moritz and Agard, 2001) has been replaced with a new model in which these three GCPs bind γ-tubulin directly, therefore being incorporated into the core ring structure (Guillet *et al.*, 2011; Kollman *et al.*, 2011).

The previous proposed model has persistently been questioned with regard to two crucial points. First, what is the mechanism by which microtubules nucleate from the γ-TuC? Second, how does the γ-TuC attach to MTOCs such as the centrosome and SPB? GCP1–6 have proved to be insufficient for answering both of these critical questions (Masuda *et al.*, 1992; Masuda and Shibata, 1996; Aldaz *et al.*, 2005; Kollman *et al.*, 2010, 2011), and therefore three other γ-TuC–interacting proteins, NEDD1/GCP-WD/GCP7, MOZART2/GCP8, and MOZART1/GIP1/GCP9, have appeared to be of particular interest (Gunawardane *et al.*, 2003; Haren *et al.*, 2006; Luders *et al.*, 2006; Hutchins *et al.*, 2010; Teixido-Travesa *et al.*, 2010; Nakamura *et al.*, 2012; Pinyol *et al.*, 2013). Among the three proteins, only MOZART1 is highly conserved in a broad range of eukaryotes, including fungi and plants (albeit not in budding yeast; Janski *et al.*, 2008, 2012; Hutchins *et al.*, 2010; Nakamura *et al.*, 2012; see Table 1), raising the possibility that this conserved protein is involved in the fundamental functions of the γ-TuC at the MTOCs.

Genetically tractable fission yeast is an ideal system to study the functions of the γ-TuC. In this yeast, GCP1–6 are all conserved (GCP1/Gtb1/Tug1, GCP2/Alp4, GCP3/Alp6, GCP4/Gfh1, GCP5/Mod21, and GCP6/Alp16; Horio *et al.*, 1991; Stearns *et al.*, 1991; Vardy and Toda, 2000; Fujita *et al.*, 2002; Venkatram *et al.*, 2004; Anders *et al.*, 2006; Table 1). Gtb1/Tug1, Alp4, and Alp6 are essential for cell viability, while the other three GCPs are dispensable, as in *Aspergillus nidulans* and *Drosophila melanogaster* (Verollet *et al.*, 2006; Xiong and Oakley, 2009). Of equal importance is the fact that human γ-tubulin is functional; the human counterpart is capable of rescuing otherwise lethal fission yeast γ-tubulin deletion mutants (Horio and Oakley, 1994). Furthermore, microtubules nucleate from multiple MTOCs besides the SPB similar to animal cells (Sawin and Tran, 2006), and the individual MTOCs are specifically activated in a

H. sapiens[a]	*X. laevis*	*D. melanogaster*	*A. thaliana*	*A. nidulans*	*S. pombe*	*S. cerevisiae*
GCP1	TUBG1, 2	γTub23C, CD	TUBG1, 2	MIPA	Gtb1/Tug1	Tub4
GCP2	Xgrip110	Dgrip84	GCP2	GCPB	Alp4	Spc97
GCP3	Xgrip109	Dgrip91	GCP3	GCPC	Alp6	Spc98
GCP4	Xgrip75	Dgrip75	GCP4	GCPD	Gfh1	
GCP5	Xgrip133	Dgrip128	GCP5	GCPE	Mod21	
GCP6	Xgrip210	Dgrip163	GCP6	GCPF	Alp16	
MOZART1	MOZART1	MOZART1	GIP1a, b[b]	MZTA	Mzt1	

[a]In humans, MOZART2A and MOZART2B were identified as new components of the γ-TuC (Hutchins *et al.*, 2010); however, these homologues are found only in the deuterostome lineage. NEDD1/GCP-WD interacts with the γ-TuC, yet appears not to be an integral component of the γ-TuC (Choi *et al.*, 2010; Nakamura *et al.*, 2012) and is not conserved in fungi. These two classes of proteins are therefore excluded from this table.
[b]GIP1a and GIP1b (Nakamura *et al.*, 2012) are also called GIP2 and GIP1, respectively (Janski *et al.*, 2012).

TABLE 1: Comparison of γ-TuC proteins in different species.

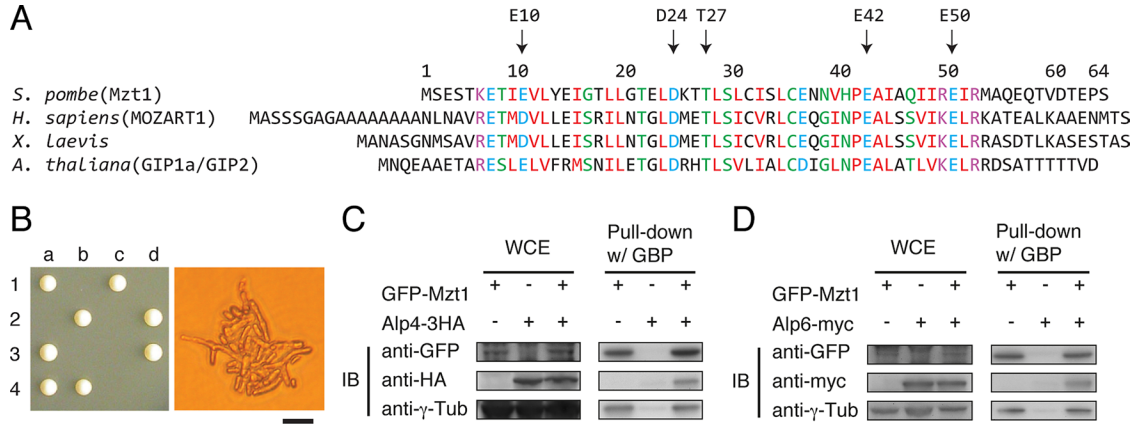

FIGURE 1: Fission yeast Mzt1 is a conserved, essential component of the γ-TuC. (A) Comparison of amino acid sequences between Mzt1 and its homologues from other species. Amino acid residues used for site-directed mutagenesis (*Materials and Methods* and Figure S2) are indicated by vertical arrows. (B) Mzt1 is essential for cell viability. Diploid cells heterozygous for *mzt1* (*mzt1*$^+$/*mzt1::natR*) were sporulated and individual spores (a–d) in each ascus (1–4) were dissected on rich media. Two viable and two nonviable segregation patterns were obtained (left), in which viable colonies were sensitive to clonNAT, meaning that these cells are *mzt1*$^+$. Microscopic observation of an *mzt1::natR* segregant showed that the *mzt1*-deleted spore germinated, divided several times, and arrested with elongated and branched morphologies (right). Scale bar: 20 μm. (C and D) Mzt1 is a component of the γ-TuC. Cells containing GFP-Mzt1 only, Alp4-3HA only, or both (C) or GFP-Mzt1 only, Alp6-13Myc only, or both (D) were grown, and protein extracts were prepared; this was followed by pull down with GBP (GFP-Trap). Immunoblotting was performed with anti-GFP, anti-HA, and anti–γ-tubulin (C) or anti-GFP, anti-Myc, and anti–γ-tubulin antibodies (D).

cell cycle–dependent manner (Masuda *et al.*, 1992; Hagan and Petersen, 2000; Sawin and Tran, 2006). Intriguingly, MOZART1 is conserved in fission yeast (Hutchins *et al.*, 2010; Table 1). In this work, we present the functional characterization of MOZART1 (called Mzt1). We have unveiled that Mzt1 plays a unique role among the γ-TuC components and is specifically required for the recruitment of the γ-TuC to the SPB, although it is dispensable for the assembly of the core γ-TuC. The conserved mechanisms underlying recruitment and attachment of the γ-TuC and microtubule nucleation are discussed.

RESULTS

The mzt1+ gene is essential for cell viability

The amino acid sequence translated from the genome sequence corresponding to the *mzt1*$^+$ open reading frame (ORF) predicted that the gene could encode two types of products, which consist of 64 and 97 amino acid residues, depending on the assignment of the initiator methionine (Supplemental Figure S1A). In this study, we defined the shorter ORF as the gene coding for Mzt1 (Figure 1A). This assignment was based on the following three criteria. First, a recent report of its transcripts proposed that the second methionine is the initiator (Bitton *et al.*, 2011). Second, the sequences of the Mzt1 homologues found in three other closely related fission yeast species—*Schizosaccharomyces cryophilus*, *Schizosaccharomyces japonicus*, and *Schizosaccharomyces octosporus*, show that Mzt1 in these species is composed of 64, 65, and 64 residues, respectively (Bechhoefer and Rhind, 2012; see Figure S1A). Finally, we found that the shorter Mzt1 protein localized to the SPB/MTOC (see Figures 2 and 3) more efficiently than the longer version (Figure S1, B and C).

We first asked whether the *mzt1*$^+$ gene plays an essential role in cell viability. To explore this possibility, we deleted one copy of the *mzt1*$^+$ gene in diploids with the PCR-mediated gene replacement method using the nourseothricin-dihydrogen sulfate (clonNAT)-resistant gene as a selectable marker (Bähler *et al.*, 1998; Sato *et al.*, 2005). clonNAT-resistant transformants were subjected to sporulation, and tetrad dissection was performed. Of the 20 asci dissected, we obtained two viable and two nonviable spores per ascus (Figure 1B, left), in which viable colonies displayed clonNAT-sensitive phenotypes (representing wild-type *mzt1*$^+$), indicating that *mzt1*$^+$ is essential for cell viability. Microscopic observation of nonviable cells showed that the spores containing the *mzt1*-deleted locus could germinate and undergo several rounds of cell division, but cells were subsequently arrested with elongated, branched morphologies (Figure 1B, right). This result shows that the *mzt1*$^+$ gene plays an essential role in successive cell division.

Mzt1 is a component of the γ-TuC

Next we addressed whether Mzt1 is a component of the γ-TuC. To this end, we tagged green fluorescent protein (GFP) into Mzt1's N-terminus prior to the initiator methionine (see *Materials and Methods*), enabling the GFP-Mzt1 protein to be produced under the control of the endogenous promoter. GFP tagging did not interfere with Mzt1 function, as a strain producing GFP-Mzt1 divided normally, comparable with a nontagged parental strain. Using this tagged construct, we created a strain that contained GFP-Mzt1 and Alp4-HA (GCP2/Spc97 homologue; Vardy and Toda, 2000). Pull down with a GFP-binding protein (GBP) showed that Mzt1 interacts with both Alp4 and γ-tubulin (Figure 1C). The pull down was then repeated with cells that instead contained GFP-Mzt1 and Alp6-Myc (GCP3/Spc98; Vardy and Toda, 2000). Again, GFP-Mzt1 pulled down Alp6-Myc and γ-tubulin (Figure 1D). Thus Mzt1 is a novel essential component of the γ-TuC in fission yeast.

Mzt1 localizes to the SPB throughout the cell cycle and to the equatorial MTOC during the postanaphase period and is present in approximately equal stoichiometry with Alp4/GCP2

Previous work showed that the γ-TuC localizes to several MTOCs within the cell in a cell cycle–dependent manner (Figure 2A). These

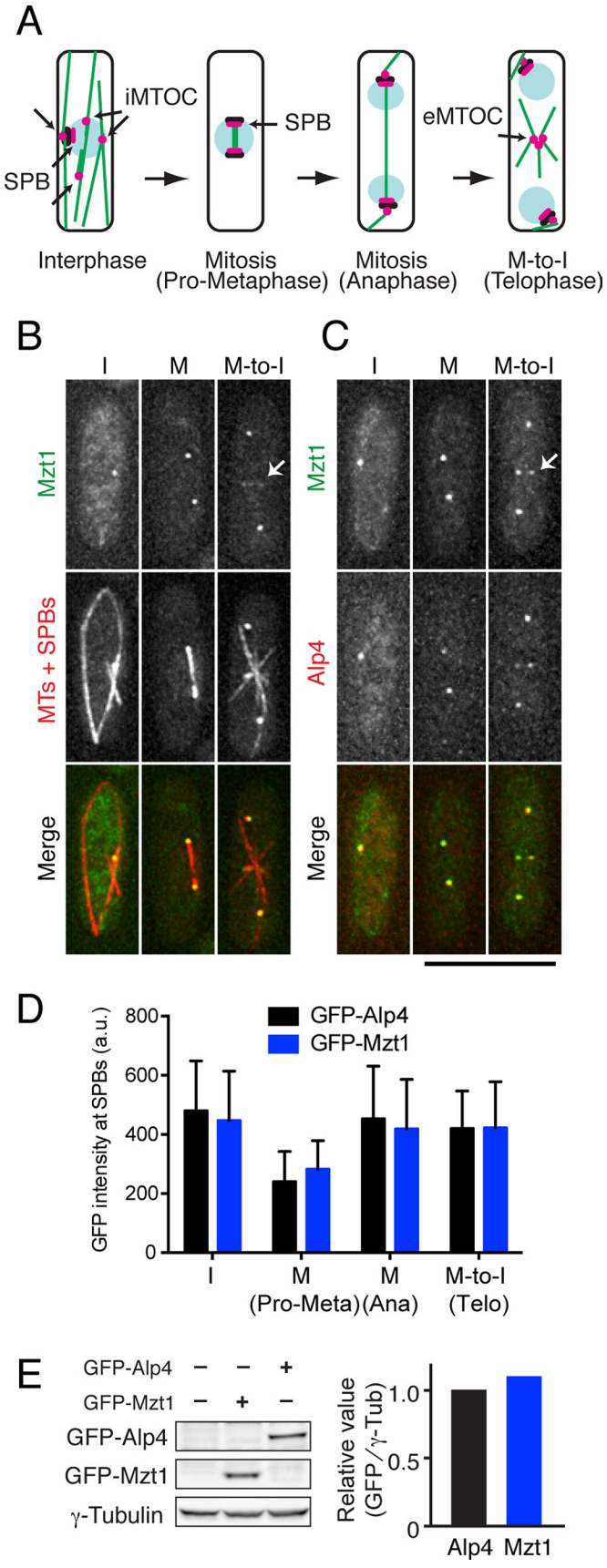

FIGURE 2: Mzt1 localizes to the SPB and the eMTOC. (A) Schematic diagram showing individual MTOCs during the fission yeast cell cycle. These include the SPB, the eMTOC, and iMTOC, corresponding to discrete dots along cytoplasmic microtubules or on the nuclear membrane. (B) Mzt1 localizes to the SPB and the eMTOC. Cells containing GFP-Mzt1 (top row) and mCh-Atb2 (MTs) and Sid4-mRFP (SPBs) (middle row) were analyzed; snapshots of interphase (I), mitotic (M), and telophase cells (M-to-I) taken from time-lapse live images are shown. Merged images are presented on the bottom (green for Mzt1 and red for MTs and SPBs). (C) Mzt1 colocalizes with Alp4/GCP2 to the SPB and the eMTOC. The same procedure was followed as in (B), except that cells containing GFP-Mzt1 (top row) and mCh-Alp4 (middle row) were used. The position of the eMTOCs is indicated with arrows. Scale bar: 10 μm. (D) Quantification of fluorescence intensities of GFP-Mzt1 and GFP-Alp4 located at the SPBs during the cell cycle. GFP signals were quantified during both interphase and each stage of mitosis (premetaphase, Pro-Meta; anaphase, Ana; telophase, Telo). (E) Quantification of Mzt1 and Alp4 protein levels in whole-cell extracts. Two strains containing GFP-Mzt1 or GFP-Alp4 and a control nontagged strain were grown at 27°C, and protein extracts were prepared. Immunoblotting was performed with anti-GFP and anti–γ-tubulin antibodies. Relative amounts of GFP-Mzt1 and GFP-Alp4 were normalized using those of γ-tubulin as a control. The relative value of GFP-Alp4 is assigned as 1.0, and that of GFP-Mzt1 is 1.1.

MTOCs include the SPB (during both interphase and mitosis), the equatorial MTOC (eMTOC) during the postanaphase period, and the interphase MTOC (iMTOC) that consists of distinct dots along the cytoplasmic microtubules or on the nuclear membrane (Horio *et al.*, 1991; Drummond and Cross, 2000; Vardy and Toda, 2000; Tran *et al.*, 2001; Fujita *et al.*, 2002; Sawin *et al.*, 2004; Venkatram *et al.*, 2004; Janson *et al.*, 2005; Zimmerman and Chang, 2005; Hoog *et al.*, 2007). To examine the precise cellular localization of Mzt1, we constructed two kinds of strains; one contained GFP-Mzt1, mCherry-tagged Atb2 (α2-tubulin, mCh-Atb2), and mRFP-tagged Sid4 (constitutive SPB component, Sid4-mRFP) (Toda *et al.*, 1984; Chang and Gould, 2000), while the other contained GFP-Mzt1 and mCherry-tagged Alp4 (mCh-Alp4). Observation of the fluorescent signals showed that Mzt1 localized to the SPB throughout the cell cycle, to the eMTOC upon mitotic exit, and, importantly, colocalization was seen with Alp4 (Figure 2, B and C; the position corresponding to the eMTOCs is marked with arrows).

For gaining insight into the stoichiometry between Mzt1 and Alp4 in the cell, the fluorescence intensities of each GFP-tagged protein detected at the SPB that was produced from individual native promoters were quantified during the cell cycle. As shown in Figure 2D, the signal intensities of these two proteins were almost equivalent during both interphase and mitosis. We also performed quantitative immunoblotting of GFP-Mzt1 and GFP-Alp4 in whole-cell extracts. Again it was evident that these two proteins are present in roughly equal quantities (a molecular ratio between Alp4 and Mzt1 is 1:1.1, Figure 2E). These data show that Mzt1 and Alp4 exist with similar stoichiometry both in soluble cell extracts and at the SPB in the cell.

Mzt1 also localizes to the interphase MTOCs

In plant cells, it was reported that a subpopulation of the γ-TuC, such as those existing on mitotic microtubules, contains MOZART1/GIP1, while the other population, such as that localizing to the cortical sites, does not (Nakamura *et al.*, 2012). This suggests that the composition of the γ-TuC may vary within individual MTOCs, depending on the presence or absence of this component. Having seen colocalization of Mzt1 with Alp4 at the SPB and eMTOC, we further observed whether Mzt1 localizes to the other MTOCs, namely the

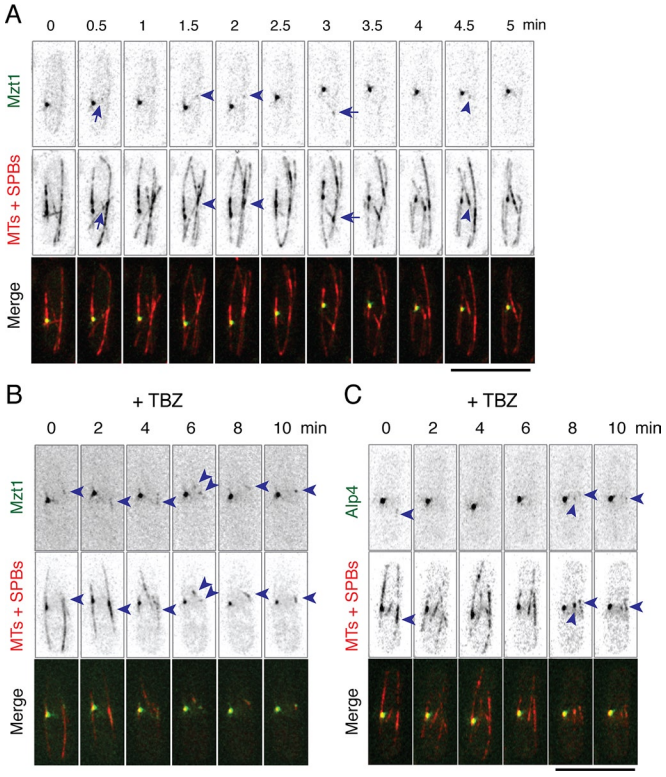

FIGURE 3: Mzt1 localizes to the iMTOC. (A) Mzt1 localizes to the interphase microtubule as punctate dots. Time-lapse live images of cells containing GFP-Mzt1 (top) and mCh-Atb2 (MTs) and Sid4-mRFP (SPBs) (middle) are shown. Merged images are presented on the bottom (green for Mzt1 and red for MTs and SPBs). In addition to the SPB, Mzt1 localizes to microtubules as dots; these dots particularly colocalize with the sites of microtubule overlapping zones (arrowheads at 1.5-, 2-, and 4.5-min time points) or microtubule branching points (arrows at 0.5- and 3-min time points). (B and C) Mzt1 and Alp4 localize to the interphase microtubule nucleation sites upon microtubule depolymerization. Cells containing mCh-Atb2 (MTs) plus Sid4-mRFP (SPBs) and GFP-Mzt1 (B) or GFP-Alp4 (C) were treated with the microtubule-depolymerizing drug TBZ (100 μg/ml) at time 0, and live imaging was subsequently performed. As microtubules depolymerized, localization of Mzt1 and Alp4 to the non-SPB sites on remnant microtubules (marked with arrowheads that correspond to the iMTOCs; Bratman and Chang, 2007) became evident. Scale bars: 10 μm.

iMTOCs that comprise punctate dots along cytoplasmic microtubules and those on the nuclear membrane (Sawin *et al.*, 2004; Janson *et al.*, 2005; Zimmerman and Chang, 2005; Sawin and Tran, 2006). Time-lapse live imaging of GFP-Mzt1 during interphase showed that, in addition to being present in the SPB, Mzt1 localized as discrete signals to the cytoplasmic microtubules (Figure 3A). Intriguingly, these punctate dots were most obvious at the microtubule overlapping zones (arrowheads at 1.5-, 2-, and 4.5-min time points) or branching points where two microtubules merged (arrows at 0.5- and 3-min time points).

To confirm that these non-SPB punctate dots correspond to the iMTOCs, we treated cells with the microtubule-depolymerizing drug thiabendazole (TBZ), and Mzt1 localization was followed as the microtubules depolymerized from their plus ends. It was previously shown that remnant microtubule sites upon microtubule depolymerization correspond to the iMTOCs (Bratman and Chang, 2007). As shown in Figure 3B, the Mzt1 signals observed not at the SPB

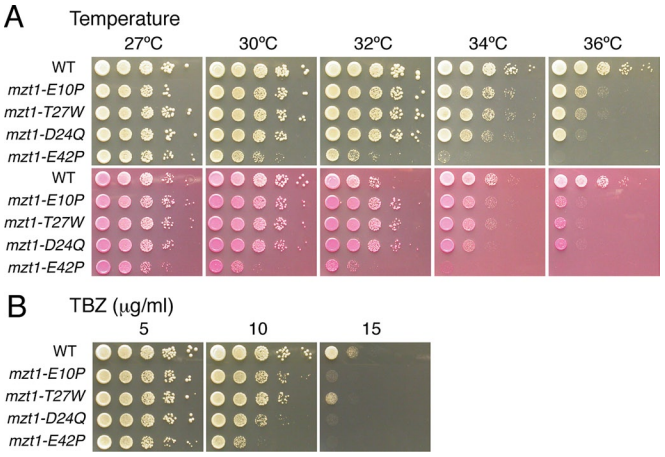

FIGURE 4: Isolation of *mzt1* ts mutants. (A and B) Serial dilution spot assay of *mzt1* ts mutants. Mutants were spotted onto rich YE5S media plates in the absence (top) or presence (bottom) of phloxine B (A) or rich media containing indicated concentrations of TBZ (B) and incubated at various temperatures for 3 d (plates containing TBZ were incubated at 27°C). Four representative alleles (*mzt1-E10P*, *mzt1-D24Q*, *mzt1-T27W*, and *mzt1-E42P*) were spotted. See Figure 1A for the positions of mutated amino acid residues.

appeared as dots localizing to the remnant microtubules and often around the nucleus (Figure 3B, arrowheads). Similarly, Alp4 localized to these remnant microtubule sites (Figure 3C, arrowheads). Taking all of these results into consideration, we conclude that, like Alp4, Mzt1 is a constitutive component of the γ-TuC that localizes to all the MTOCs throughout the cell cycle.

Temperature-sensitive *mzt1* mutants display interphase microtubule defects at the permissive temperature

To examine the roles of Mzt1 in cell division and microtubule assembly, we constructed several temperature-sensitive (ts) mutants of *mzt1*. For this purpose, multiple amino acid residues conserved across various species were selected and mutated individually to other random amino acids by PCR-based, site-directed mutagenesis (see Figure 1A for amino acid residues mutagenized, and *Materials and Methods* and Supplemental Figure S2 for experimental procedures). Figure 4A shows a serial dilution spot assay of four temperature-sensitive mutants isolated (*mzt1-E10P*, *mzt1-D24Q*, *mzt1-T27W*, and *mzt1-E42P*). Note that similar to previously isolated mutants of γ-TuC components (Vardy and Toda, 2000; Fujita *et al.*, 2002), *mzt1* mutants were hypersensitive to TBZ (Figure 4B).

Close inspection of the microtubules and SPBs (mCh-Atb2 and Sid4-mRFP) in the *mzt1-T27W* mutant showed that mutant cells appeared to contain a reduced number of interphase microtubule bundles, even when grown at the permissive temperature (27°C; Figure 5, A and B). Quantification showed that the number of bundles was indeed significantly reduced: ~1.8 bundles per mutant compared with 4.5 per wild-type cell (Figure 5C). Similar interphase microtubule defects were also observed in the *mzt1-E10P* or *mzt1-D24Q* mutants. The appearance of these abnormal interphase microtubules is reminiscent of mutants of the γ-TuC components (Paluh *et al.*, 2000; Vardy and Toda, 2000; Hendrickson *et al.*, 2001; Fujita *et al.*, 2002; Sawin *et al.*, 2004; Venkatram *et al.*, 2004; Zimmerman and Chang, 2005; Anders *et al.*, 2006; Masuda *et al.*, 2006a). Measurement of GFP-Alp4 signals at the interphase SPB in these *mzt1* mutant cells showed that the fluorescence signals were already substantially reduced at the permissive temperature, with ~95% reduction at interphase SPBs

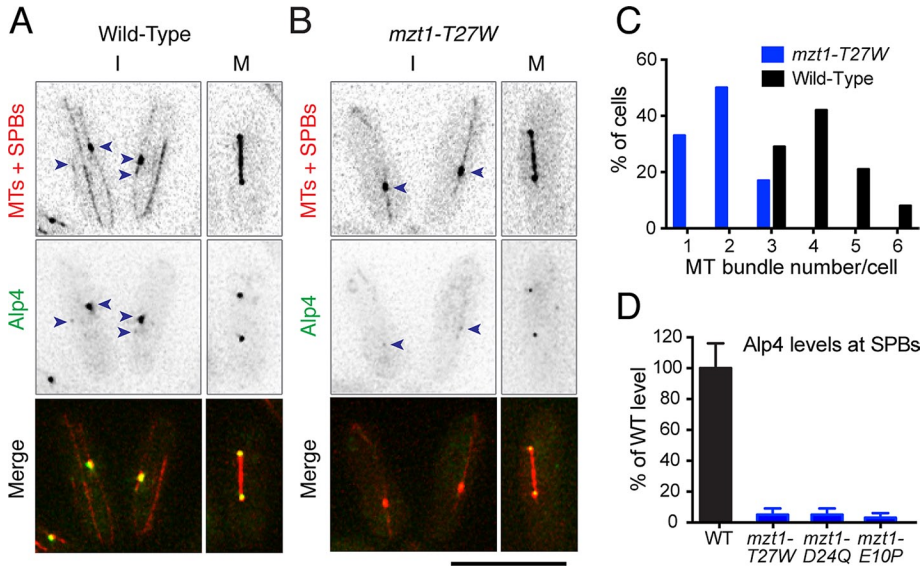

FIGURE 5: *mzt1* ts mutants are defective in interphase microtubule organization at the permissive temperature. (A and B) Morphology of interphase and mitotic spindle microtubules at the permissive temperature. Snapshots of microtubule structures in wild-type (A) or *mzt1-T27W* mutant (B) cells containing mCh-Atb2 (MTs), Sid4-mRFP (SPBs, top), and GFP-Alp4 (middle) are shown during interphase (I, left) and mitosis (M, right). Cells were grown in rich media at 27°C. SPBs (Wild-Type and *mzt1-T27W*) and iMTOCs situated on microtubules (Wild-Type) are indicated with arrowheads. Scale bar: 10 μm. (C) The number of interphase microtubules. The interphase microtubule bundles were counted for wild-type and *mzt1-T27W* mutant cells ($n = 24$) grown at 27°C. (D) Alp4 signal intensities at the interphase SPB. Signal intensities of Alp4 at the interphase SPB were measured in three alleles of *mzt1* ts mutants (*mzt1-T27W*, *mzt1-D24Q*, and *mzt1-E10P*) that contain GFP-Alp4, mCh-Atb2, and Sid4-mRFP. Values were compared with those of wild-type cells ($n = 53$–88 per each sample).

in all three *mzt1* mutant alleles (Figure 5D). Also of note was that we were unable to visualize the iMTOC or eMTOC in these mutants (Figure 5B). We envisage that the reduced γ-TuC levels at the MTOCs during interphase leads to the appearance of interphase microtubule defects at this temperature. Furthermore, like other γ-TuC mutants (Paluh *et al.*, 2000; Vardy and Toda, 2000; Fujita *et al.*, 2002; Sawin *et al.*, 2004; Venkatram *et al.*, 2004; Zimmerman and Chang, 2005; Masuda *et al.*, 2006a), *mzt1-T27W* cells showed bent morphology, even at the permissive temperature (Figure 5B, right), and this defect became more exaggerated at the restrictive temperature (see Figure 7, B and C, later in the paper).

Mzt1 is required for bipolar mitotic spindle microtubules and chromosome segregation

Observation of mitotic *mzt1-T27W* cells incubated at 36°C revealed characteristic defects in spindle microtubule formation and chromosome segregation (designated types I and II, Figure 6, A–D). Of mitotic cells, 47% ($n = 30$) displayed a significant delay in SPB separation and spindle elongation during early mitosis (Figure 6B, type I. For comparison, a cell exhibiting normal mitotic progression is shown in Figure 6A). In this type of cells, the two SPBs failed to separate toward the cell tips for a duration of more than 20 min, during which they often became spatially closer again. This phenotype, called SPB convergence or spindle collapse, is reminiscent of failure in bipolar spindle formation (Hauf *et al.*, 2007; Hsu and Toda, 2011). Indeed, the spindle microtubules that normally connect the two separating SPBs were dim, with only the two SPB dots clearly visible. In addition, during this period, the chromosomes (CFP-tagged histone H3, Hht1-CFP) never segregated (Figure 6B, top row), indicating this cell underwent mitotic delay with unattached kinetochores. This indicates that Mzt1 is required to form stable spindle microtubules. Presumably, this defect is directly ascribable to the role of Mzt1 in nucleation of mitotic spindle microtubules from the SPB.

In the second category (20%, $n = 30$, type II), lagging, chromosome-like phenotypes were observed during mid- to late mitosis (Figure 6C, top row, evident at 12 min). Unlike the previous type I cells (Figure 6B), apparently normal spindle microtubules were formed and elongated (middle row). We envision that spindle–kinetochore interaction at the plus end of spindle microtubules is somehow compromised in type II mitotic cells, leading to chromosome segregation defects. The *mzt1-E10P* mutant also displayed similar phenotypes, although the percentage of types I and II varied from that of *mzt1-T27W* cells (14% type I and 53% type II; Figure 6D). Collectively Mzt1 is necessary for the proper assembly of both interphase and mitotic spindle microtubules that is essential for accurate chromosome segregation.

Mzt1 is required for localization of the γ-TuC to the mitotic SPB, and the quantity of the remaining γ-TuC accounts for the varied phenotypic outcomes

Previous results suggested that Mzt1 may play dual roles in microtubule organization during mitosis: nucleation from the SPB (type I) and kinetochore-microtubule interaction at the plus end (type II). Although spindle microtubules were formed and elongated, it is possible that microtubule organization in type II cells is in fact somewhat defective. To address why and how these two different phenotypes arose, we quantified the fluorescence intensities of Alp4 (GFP-Alp4) and spindle microtubules (mCh-Atb2) in wild-type and each type of *mzt1-T27W* cells under time-lapse microscopy. At 1.5 h after temperature shift up from 27°C to 36°C, late G2 cells (cells longer than 13 μm) were chosen under the microscope, and subsequent mitotic progression was filmed.

Live images of representative cells of wild type (Figure 7A), type I (Figure 7B), and type II (Figure 7C) are shown (note that 0 min is defined by the time point when SPBs started to separate, which is a landmark for mitotic entry). At each time point, fluorescence intensities of Alp4 (at both SPBs) and spindle microtubules were measured. It was found that the intensities of both Alp4 (Figure 7D) and microtubules (Figure 7E) were substantially reduced in both types of *mzt1-T27W* mutant cells. Average signal intensities relative to those of wild-type cells over the time course are shown in Figure 7F. Intriguingly, type I cells consistently exhibited a more drastic reduction of intensities in both Alp4 and microtubules than type II cells. While a ~90% (Alp4) and ~75% (microtubules) reduction was observed in type I cells, type II cells displayed ~80% (Alp4) and ~60% reduction (microtubules), respectively (Figure 7F). In contrast, the reduction of signal intensities at the permissive temperature was modest, with ~70% for Alp4 and ~50% for microtubules.

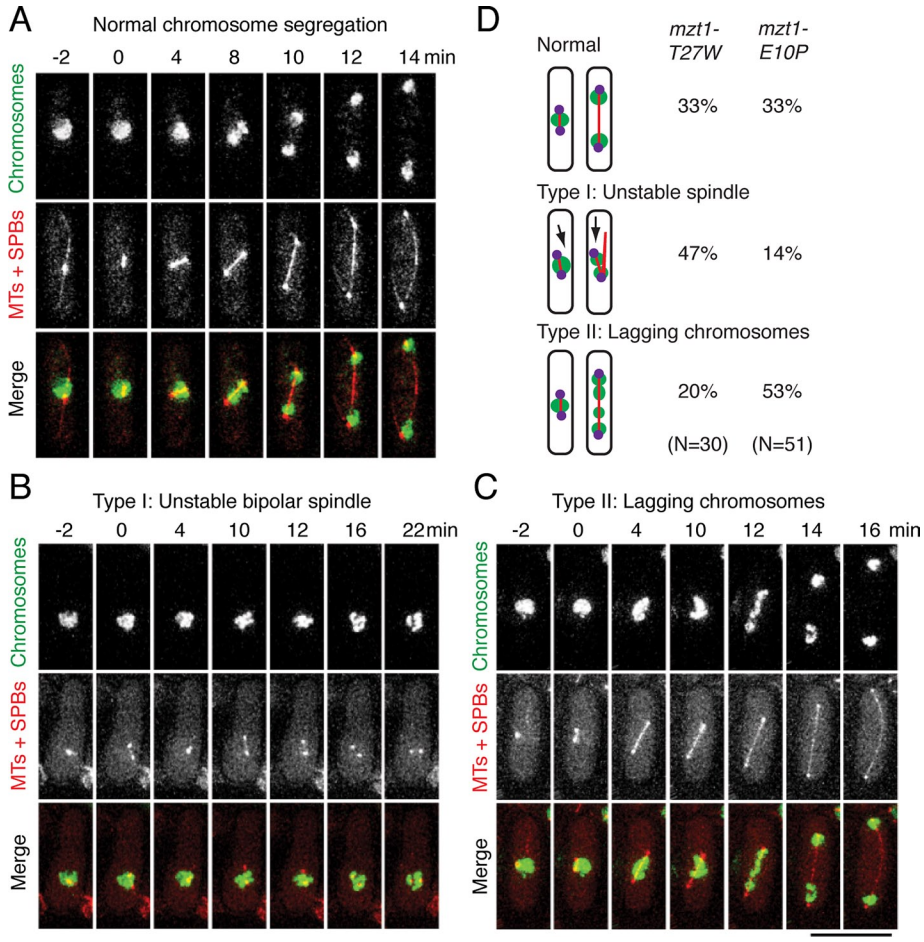

FIGURE 6: Two different mitotic defects appear in the *mzt1* mutant. (A–C) Mitotic phenotypes of *mzt1* ts mutants. Time-lapse live images of *mzt1-T27W* cells corresponding to each representative phenotype are presented; mitotic cells displaying normal spindle formation and elongation and chromosome segregation (A), type I cells displaying unstable spindle microtubules (B), and type II cells exhibiting the lagging, chromosome-like phenotype with apparently normal morphologies of spindle microtubules (C). *mzt1-T27W* mutant cells containing Hht1-CFP (histone H3, chromosomes, top) and mCh-Atb2 (MTs) and Sid4-mRFP (SPBs) (middle) were grown at 27°C; this was followed by a temperature shift up to 36°C. Merged images are presented on the bottom (green for chromosomes and red for MTs and SPBs). Cells were imaged starting from 2 h later. Scale bar: 10 μm. (D) Classification and quantification of mitotic phenotypes. The data of two *mzt1* mutant alleles (*mzt1-E10P* and *-T27W*) are shown, type I cells exhibit unstable spindle microtubules, whereas type II cells show the lagging, chromosome-like phenotype.

Results obtained from this experiment indicated that the amount of Alp4 (the γ-TuC) at the mitotic SPBs, which is also proportional to microtubule intensity, correlates with the phenotypic appearance of *mzt1-T27W* cells (Figure 7G). Importantly, this analysis also demonstrated that Mzt1 is critical for the recruitment and/or retention of the core γ-TuC to the mitotic MTOC. We conclude that Mzt1 is required for the attachment of the γ-TuC to the MTOCs.

Mzt1 is dispensable for the formation of the core γ-TuC

Results thus far show that Mzt1 is a constitutive component of the γ-TuC that plays a crucial role in the recruitment and/or retention of the γ-TuC to the MTOCs. We next asked in which step Mzt1 plays a decisive role in γ-TuC function. Two scenarios immediately arise, although they are not mutually exclusive. In one scenario, Mzt1 is a recruiting factor of the γ-TuC to the MTOCs. In the other scenario, Mzt1 is required for complex formation or maintaining the integrity of the γ-TuC, a prerequisite for γ-TuC localization to the MTOCs. To distinguish between these two possibilities, we performed a pull-down assay in *mzt1-T27W* and *mzt1-D24Q* mutant cells that contained GFP-Alp4. If the latter scenario was true, interaction between Alp4 and γ-tubulin would be abolished at 36°C. As shown in Figure 8A, it was found that Alp4 was still able to form a complex with γ-tubulin, and indeed, quantification of the amount of γ-tubulin pulled down with GFP-Alp4 was not lessened in either of the *mzt1* mutants incubated at the restrictive temperature (Figure 8B). From this result, we favor the notion that Mzt1 is not required for assembly of the γ-TuC, but instead it is specifically needed for the γ-TuC to be recruited and/or tethered to the SPB.

Mzt1 localization to the SPB requires a core component of the γ-TuC

We next sought to examine whether Mzt1 localization to the SPB in turn requires integrity of the γ-TuC. Namely, we asked whether Mzt1 alone is sufficient for its localization to the SPB independently of the other essential components of the γ-TuC. To this end, we used the *alp6-719* ts mutant (Vardy and Toda, 2000). Previous work showed that this mutation leads to the disappearance of Alp4 from the SPB when incubated at the restrictive temperature (Venkatram *et al.*, 2004). The *alp6-719* mutants containing GFP-Mzt1 or GFP-Alp4 were each constructed (with mCh-Atb2 and Sid4-mRFP), and the fluorescence intensities of Mzt1 and Alp4 were quantified upon incubation at 36°C. As shown in Figure 9, A and B, it was evident that the intensities of both GFP-Alp4 and GFP-Mzt1 declined noticeably upon 1-h incubation and were further reduced after 2-h incubation.

Quantification of GFP signal intensities confirmed that Alp4 and Mzt1 levels at the SPB were substantially reduced during both interphase and mitosis by 83–93% upon 2-h incubation at the restrictive temperature (Figure 9C). It is noted that the degree of reduction was almost indistinguishable between Mzt1 and Alp4. This result demonstrated that Mzt1 localization to the SPB requires structural integrity of the core γ-TuC. Taking these results together, we consider that, in fission yeast, only the core γ-TuC consisting of Alp4, Alp6, Mzt1, and γ-tubulin can localize to the SPB.

DISCUSSION

In the current study, we show that fission yeast Mzt1 is an essential, stoichiometric component of the γ-TuC, which localizes to all the MTOCs throughout the cell cycle. We further show that Mzt1 is required for γ-TuC localization to the SPB, although not for the assembly of the core γ-TuC. Hence, Mzt1 plays a hitherto unknown unique role among the γ-TuC core components, in that it is specifically required for the recruitment and/or attachment of this complex to the major MTOC site.

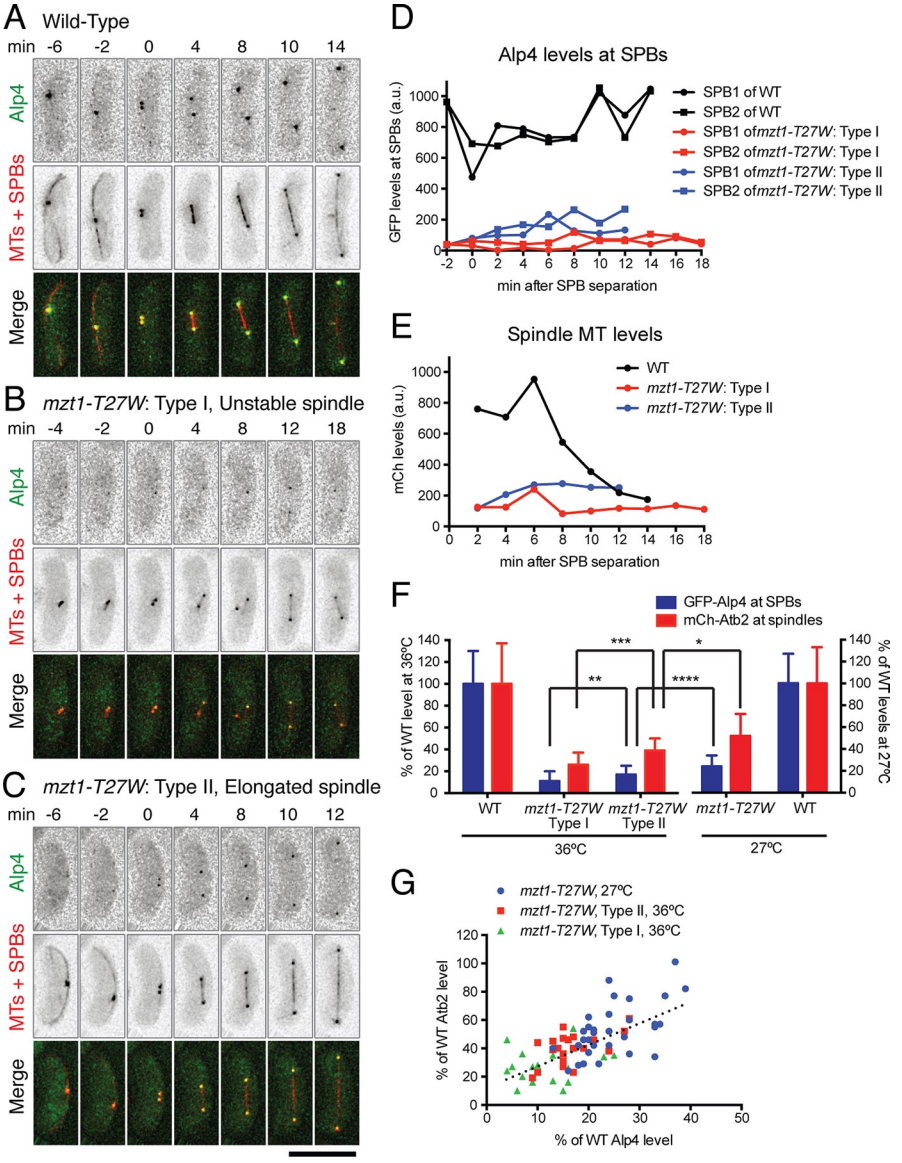

FIGURE 7: Mzt1 is required for Alp4 localization to the SPB and the residual Alp4 levels correlate with the phenotypic differences. (A–C) Time-lapse live imaging of microtubules, SPBs, and Alp4. Wild-type (A) or *mzt1-T27W* mutant (B and C) cells containing GFP-Alp4 (top) and mCh-Atb2 (MTs) and Sid4-mRFP (SPBs) (middle) were grown at 27°C; this was followed by a temperature shift up to 36°C. Merged images are presented on the bottom (green for Mzt1 and red for MTs and SPBs). Time-lapse imaging was started 1.5 h later. The time point when the two SPBs started to separate was assigned as mitotic entry (0 min). Note that *mzt1-T27W* mutant cells became bent, reminiscent of defective phenotypes seen in γ-TuC mutants (B and C). Scale bar: 10 μm. (D) Quantification of Alp4 signal intensities at the SPBs. GFP-Alp4 signals were quantified at each time point in wild-type (A), type I (B), and type II (C) cells. (E) Quantification of microtubule (MT, mCh-Atb2) signal intensities. The same procedures were followed as in (D), except that signal intensities of mCh-Atb2 were quantified. (F) Summary of Alp4 levels at the mitotic SPBs and Atb2 levels at the mitotic spindle microtubules in the *mzt1-T27W* mutant. Signal intensities of GFP-Alp4 and mCh-Atb2 corresponding to time points from 2 min to 8 min shown after SPB separation are averaged in wild-type and type I and II cells incubated at 36°C (n = 39–60 for GFP-Alp4; n = 20–24 for mCh-Atb2). Corresponding values obtained from mutant cells and wild-type cells grown at 27°C (n = 66 and 74 for GFP-Alp4; n = 32 and 36 for mCh-Atb2) are also shown. The mean values of wild-type cells were assigned as 100%. Statistical significance was determined by Student's t test. (G) Correlation of Alp4 levels at the mitotic SPBs, spindle intensities and phenotypic variations in the *mzt1-T27W* mutant. The sums of Alp4 levels from the two SPBs of mitotic spindles were plotted against Atb2 levels of the spindle microtubules in *mzt1-T27W* cells incubated at 27°C (n = 32, blue circles), or type I (n = 18, green triangles) or type II (n = 20, red squares) cells incubated at 36°C. The mean values of wild-type cells were assigned as 100%. A linear regression line is shown as a dotted line.

The structural composition of the γ-TuC within individual MTOCs

In plants and possibly some animal cells, the component composition of the γ-TuC is not uniform and may vary within the individual MTOCs (Kollman *et al.*, 2011; Nakamura *et al.*, 2012). Our results presented in this study support the notion that, instead, in fission yeast, four essential proteins, Mzt1/MOZRT1, Alp4/GCP2, Alp6/GCP3, and γ-tubulin, are constitutive components of all the MTOCs, including the SPB, eMTOC, and iMTOC (Figures 2 and 3). However, we could not rule out the possibility that the composition of the γ-TuC might in fact vary due to the heterogeneity of the other nonessential components (Gfh1/GCP4, Mod21/GCP5, and Alp16/GCP6), which is a proposal that has been previously discussed (Choi *et al.*, 2010; Kollman *et al.*, 2011). Lower abundances of these three GCPs compared with the core components (~0.1; Fujita *et al.*, 2002) render this investigation technically difficult. In terms of protein quantities, the γ-TuC contains approximately equal amounts of Mzt1 and Alp4/GCP2 (Figure 2). This substantiates the notion that Mzt1 is a constitutive, stoichiometric component of the γ-TuC.

Phenotypic variations arising from defects in Mzt1 and γ-TuC integrity

Characterization of the *mzt1* ts mutants indicated that Mzt1 is required for recruitment/attachment of the γ-TuC to the MTOCs. Furthermore, the quantitative level of γ-TuC retained at these sites in the mutants appears to be a critical determinant for the varied phenotypes that emerge. During interphase, we have observed a significant reduction of the cytoplasmic microtubule number in the *mzt1* ts mutants that is accompanied by the substantial decrease of the γ-TuC from the SPB, iMTOC, and eMTOC (Figure 5). The residual γ-TuC at the MTOCs may be responsible for low-level nucleation of cytoplasmic microtubules. On the other hand, two different phenotypes arose during mitosis (Figure 6). Type I mutant cells that retained ~10% of γ-TuC levels at the SPB could not form stable bipolar spindle microtubules, resulting in arrest during mitosis at the restrictive temperature. Type II cells that retained ~20% of γ-TuC levels assembled spindles and proceeded through mitosis, although displaying the lagging, chromosome-like phenotype (Figure 7). Our previous work has shown that *alp4-1891* mutants that lost the γ-TuC almost completely from the mitotic SPB exhibited the emergence of monopolar spindles (Vardy and Toda, 2000; Vardy *et al.*, 2002), although, interestingly, a

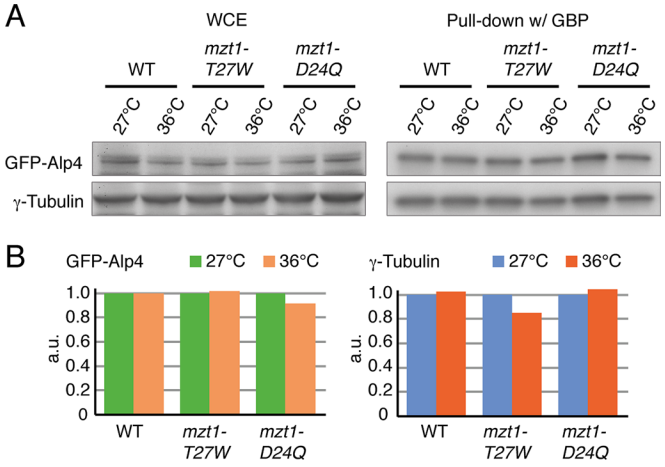

FIGURE 8: Mzt1 is not required for the formation of the core γ-TuC. (A) Wild type and two alleles of *mzt1* ts mutants (*mzt1-T27W* and *mzt1-D24Q*) that contained GFP-Alp4 were grown at 27°C and shifted to 36°C. At 0 and 2-h time points, cell extracts were prepared, and pull down was performed using GFP-Trap. Whole-cell extracts (WCE, left) and immunoprecipitates (right) were run on SDS–PAGE, and immunoblotting was performed with anti-GFP (top) or anti–γ-tubulin antibodies (bottom). Experiments were repeated twice, and the same results were obtained. (B) Quantification of the amount of GFP-Alp4 and γ-tubulin in immunoprecipitates. Immunoblotting data shown in (A) were quantified and calibrated. Relative intensities of GFP-Alp4 (left) or γ-tubulin (right) at 27°C were assigned as 100% in each strain. Note that γ-tubulin still formed a complex with Alp4 in two *mzt1* mutants as efficiently as in wild-type cells at the restrictive temperature.

modest population of *alp4-1891* cells gave rise to the type I phenotype (Masuda *et al.*, 2006b). By contrast, if ~30% of Alp4 was retained, cells managed to undergo normal mitosis, despite cytoplasmic microtubule defects (Figures 5 and 7).

Given the appearance of these different phenotypes, we propose that, during both interphase and mitosis, the γ-TuC regulates multiple aspects of microtubule organization and functions ranging from microtubule nucleation, assembly of proper mitotic spindles, and attachment of the plus end of spindle microtubules to the kinetochore. The emergence of the lagging, chromosome-like phenotype with apparently normal morphologies of spindle microtubules is intriguing; this type of mitotic defect was not reported in other mutants of the γ-TuC components (Vardy and Toda, 2000; Vardy *et al.*, 2002; Hendrickson *et al.*, 2001; Masuda *et al.*, 2006b), except for one particular mutant allele of γ-tubulin (*gtb1-PL302*) during mitosis (Paluh *et al.*, 2000) and meiosis (Tange *et al.* 2004). As the densities of spindle microtubules in this type of cells decrease (Figure 7), failure to maintain proper attachment of the kinetochores to spindle microtubules could be attributed to the reduced number of microtubule plus ends. An alternative possibility, although not mutually exclusive, is that the γ-TuC, in particular Mzt1, may play a direct or indirect role in the regulation of microtubule dynamics at the plus end, which is an issue that remains unresolved in the field (Zimmerman and Chang, 2005; Bouissou *et al.*, 2009; Anders and Sawin, 2011; Tanaka *et al.*, 2012).

Roles of fission yeast MOZART1 in γ-TuC structure and function

The requirement of Mzt1 for γ-TuC localization to the SPB raised an intriguing possibility that Mzt1 may play a specific role in the attachment of the γ-TuC to this MTOC site independent of interaction with the other γ-TuC components (Figure 7). However, subsequent experiments using *alp6-719* ts mutants (Vardy and Toda, 2000; Venkatram *et al.*, 2004) clearly indicated that Mzt1 (and Alp4) localization to the SPB was substantially impaired in this mutant (Figure 9). Accordingly, we deem Mzt1 to be capable of attaching to the SPB only when it forms a stable γ-TuC with other components (Figure 10A). By contrast, Alp4/GCP2 still interacts normally with γ-tubulin in the absence of Mzt1 function (Figure 8), indicating that Mzt1 plays no major roles in the formation of a core γ-TuC structure (Figure 10, B and C). It is of note that human MOZART1 and plant GIP1 also play a critical role in γ-tubulin localization to the MTOCs (Hutchins *et al.*, 2010; Janski *et al.*, 2012), suggesting that the molecular role of MOZART/Mzt1 in the recruitment of the γ-TuC to the MTOC is conserved through evolution.

It is known that two long coiled-coil SPB components, Mto1 and Pcp1, act as specific attachment factors for interphase cytoplasmic MTOCs (Mto1) and mitotic nuclear SPBs (Pcp1) (Sawin *et al.*, 2004; Venkatram *et al.*, 2004; Zimmerman and Chang, 2005; Fong *et al.*, 2010). Mto1 and Pcp1 belong to a conserved centrosomal/SPB protein family, the members of which include human CDK5RAP2, CG-NAP, and pericentrin; fly Centrosomin; and budding yeast Spc110, which are all known to play a crucial role in γ-TuC attachment to the centrosome/SPB (Takahashi *et al.*, 2002; Zimmerman *et al.*, 2004; Sawin *et al.*, 2004; Zhang and Megraw, 2007; Fong *et al.*, 2008; Choi *et al.*, 2010). Although these proteins physically interact with the γ-TuC, they are not regarded as integral γ-TuC components and localize to the centrosome/SPB independent of the γ-TuC. It is shown that a conserved motif found within these members, called CM1/CNN1/γ-TuNA, is responsible for binding to the γ-TuC (Zhang and Megraw, 2007; Samejima *et al.*, 2008; Barr *et al.*, 2010; Choi *et al.*, 2010). However, the precise molecular details regarding the interaction between CM1 and the γ-TuC remain to be determined. It is possible that Mzt1 is spatially exposed toward the outer interface when incorporated into the γ-TuC, thereby being capable of interacting as a bridge with the CM1 motif of these SPB/centrosomal proteins.

It has been suggested that γ-TuC attachment to the MTOCs alone may not suffice for its ability to nucleate microtubules; these two events may rely on different mechanisms, yet they are regulated coordinately (Kollman *et al.*, 2010). It was recently further proposed that, for the γ-TuC to promote microtubule nucleation, a specific conformational alteration within GCP3 (i.e., the straightening of an internal hinge) needs to be induced (Guillet *et al.*, 2011). The currently proposed structural model of either γ-TuSC or γ-TuRC does not include MOZART1 (Kollman *et al.*, 2011). Given that the MOZART1 orthologues, unlike the other GCPs, do not contain the γ-tubulin–binding GRIP 1 and 2 domains; that plant MOZART1/GIP1 directly binds GCP3 (Janski *et al.*, 2008, 2012; Nakamura *et al.*, 2012); and finally, that Mzt1 and Alp4/GCP2 are present in roughly equal quantities (Figure 2), it would be tempting to speculate that direct stoichiometric binding of MOZART1 to GCP3 results in allosteric changes within this GCP, which not only leads to the recruitment of the γ-TuC to the SPB but also is involved in promotion of microtubule nucleation, possibly via interaction with Mto1/Pcp1 attachment factors.

MATERIALS AND METHODS

Strains, media, and genetic methods

All fission yeast strains used throughout this study are listed and described in Supplemental Table S1. Fission yeast cells were grown and maintained in standard conditions as described by Moreno *et al.* (1991). Serial-dilution spot tests were carried out by spotting

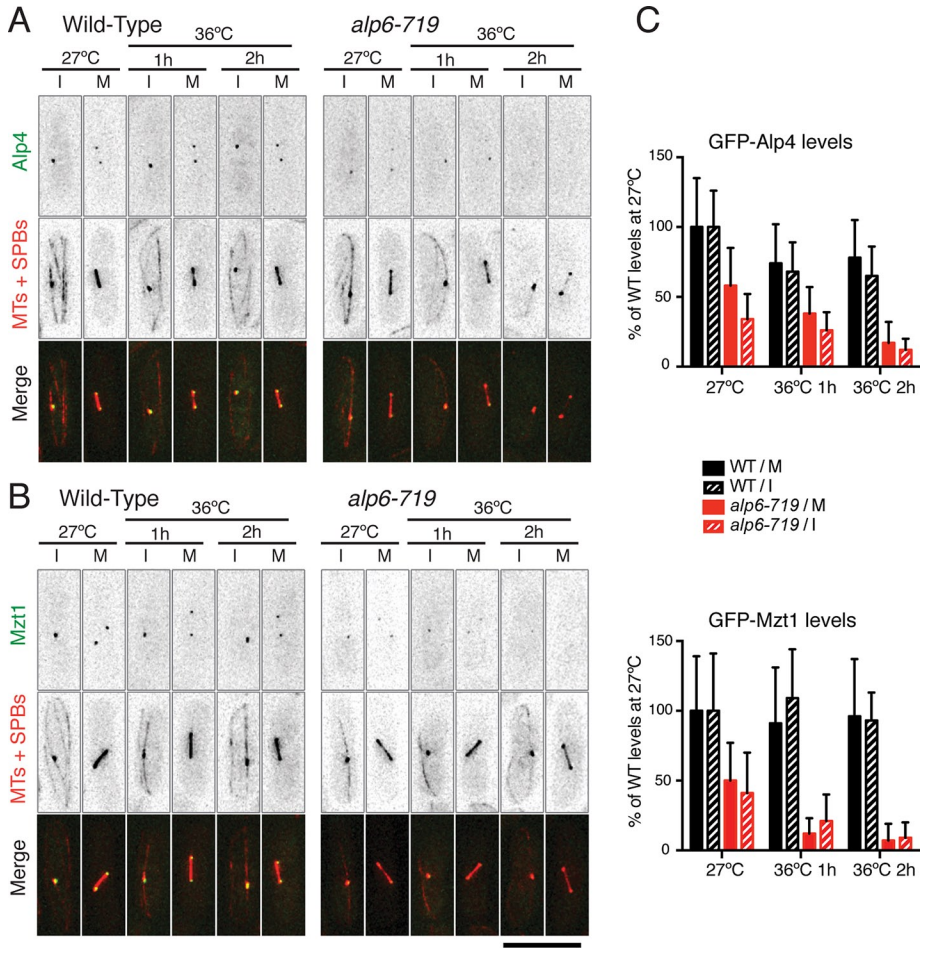

FIGURE 9: Integrity of the γ-TuC is required for Mzt1 localization to the SPB. (A) Alp4 delocalizes from the SPB in the *alp6-719* ts mutant. Wild type (left) or *alp6-719* ts mutant (right) that contained GFP-Alp4 (top) and mCh-Atb2 (MTs) and Sid4-mRFP (SPBs) (middle) were grown at 27°C and shifted to 36°C. Merged images are presented on the bottom (green for Alp4 and red for MTs and SPBs). At 0 and 1- and 2-h time points, both interphase (I) and mitotic cells (M) were filmed. Representative examples are shown in each case. (B) Mzt1 delocalizes from the SPB in the *alp6-719* ts mutant. The same procedures were followed as in (A), except that strains containing GFP-Mzt1 rather than GFP-Alp4 were used. Scale bar: 10 μm. (C) Quantification of GFP-Alp4 and GFP-Mzt1 in the *alp6-719* mutant cells. Signal intensities of GFP-Alp4 and GFP-Mzt1 were measured in both interphase and mitotic cells (shown in A and B, $n = 16–65$). Note that after 2-h incubation at 36°C, GFP-Mzt1 signals were barely detectable (7% for M and 9% for I), similar to the case of GFP-Alp4 (17% for M and 12% for I).

10-fold serial dilutions from cells at a concentration of 2×10^7 cells/ml onto plates containing either rich YE5S media or rich media with added phloxine B (7.5 μg/ml). The plates were incubated at the necessary temperature within the range of 27 to 36°C.

Nucleic acids preparation and manipulation

Enzymes were used as recommended by the suppliers (New England Biolabs, Ipswich, MA; and Takara Bio, Europe, Saint-Germain-en-Laye, France).

Gene disruption and the N-terminal and C-terminal epitope tagging

A PCR-based gene-targeting method (Bähler *et al.*, 1998) was used for complete gene disruption and epitope tagging (GFP, 3HA, mCherry) in the C- or N-terminus under the endogenous promoter. The *mzt1*$^+$ gene was deleted in diploid cells with the clonNAT-resistance marker gene (*natR*; Sato *et al.*, 2005).

For N-terminal GFP tagging of Mzt1, the *hphR* cassette from pCR2.1-hph (Sato *et al.*, 2005) was first integrated into the position at 100 base pairs upstream of the *mzt1*$^+$ORF. The resultant strain (HR2296) grew normally, indicating that insertion of the cassette did not affect Mzt1 function. Using the genomic DNA isolated from this strain and a GFP-encoding vector DNA as templates, we used PCR to construct the DNA fragment containing the *hphR* cassette, its 540–base pair upstream region, the 99–base pair 5′ upstream of *GFP-mzt1*$^+$ (*mzt1*$^+$ promoter region), *GFP-mzt1*$^+$, and the 500–base pair 3′-downstream, and this fused PCR product (*hphR-GFP-mzt1*$^+$) was used for transformation to replace the authentic *mzt1*$^+$ gene.

For construction of strains carrying GFP-Alp4 and mCherry-Alp4, the promoter region of *alp4*$^+$ was PCR-amplified and inserted at the *Bam*HI site between a selection marker *kanR* and *GFP* of pCSS25 (a gift of Yuji Chikashige, Advanced ICT Research Institute, Kobe, Japan) or mCherry of pCSS25-mCh (constructed by replacing GFP of pCSS25 with mCherry). The *alp4*$^+$ gene was replaced with *kanR-GFP-alp4*$^+$ or *kanR-mCherry-alp4*$^+$, using the vectors as templates for PCR-based gene targeting.

Isolation of temperature-sensitive *mzt1* mutants

The detailed experimental scheme for isolating *mzt1* ts mutants is summarized in Supplemental Figure S2. The PCR primers used are listed in Supplemental Table S2. Briefly, the template DNA for mutagenizing PCR containing the *mzt1*$^+$ upstream region of 640 base pairs, the *mzt1*$^+$ gene, the *hphR* cassette, and the downstream region of 330 base pairs (*URS-mzt1*$^+$*-hphR-DRS*; Figure S2A) was constructed by fusion PCR, using PCR products amplified from *Schizosaccharomyces pombe* genomic DNA and pCR2.1-hph (Sato *et al.*, 2005). Primers for site-directed mutagenesis were designed to replace the target amino acids randomly with others (Figure S2B). The following conserved residues, E10, D24, E42, E50, and T27L28S29 (Figure 1A), were specifically targeted for mutagenesis. The DNA fragments containing the mutagenized *mzt1* gene and the *hphR* cassette were obtained by fusion PCR (Figure S2C). The *S. pombe* cells (HR1758, Table S1) were transformed at 27°C with the DNA fragments on plates containing YE5S rich media and hygromycin B (0.3 mg/ml). The colonies showing temperature-sensitive growth at 36°C were isolated, and the mutations on the targeted amino acids were confirmed by nucleotide sequencing of the *mzt1* gene (Figure S2D).

Fluorescence microscopy, time-lapse live-cell imaging, and quantification

Fluorescence microscope images were obtained using the DeltaVision microscope system (Applied Precision, Seattle, WA) with a cooled charge-coupled device camera CoolSNAP.HQ

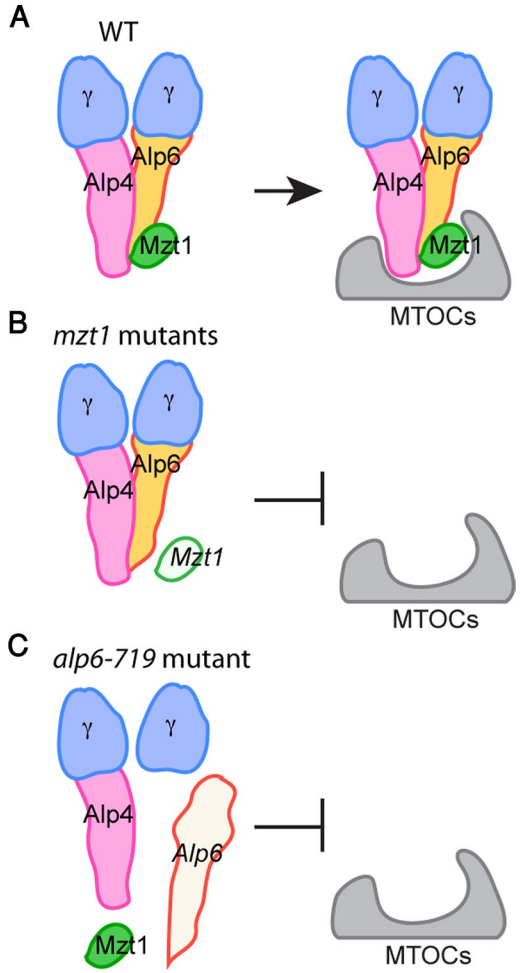

FIGURE 10: A proposed model for Mzt1 function. (A) In wild-type cells (WT), Mzt1 forms a stable, stoichiometric complex with the other core components (γ-tubulin/GCP1, Alp4/GCP2, and Alp6/GCP3) of the γ-TuC. It is essential for cell viability and γ-TuC attachment to the SPB/MTOCs. With regard to Mzt1's molecular functions, we envision the following two, albeit not mutually exclusive, scenarios. First, Mzt1 facilitates γ-TuRC formation, which leads to the recruitment/attachment of this complex to the MTOCs. Second, Mzt1 is required for the recruitment of the γ-TuC and/or γ-TuRC to the MTOCs. For simplicity, nonessential γ-TuC components (Gfh1/GCP4, Mod21/GCP5, and Alp16/GCP6) are omitted from this figure. Of note is that it is currently unknown as to how Mzt1 interacts with the core γ-TuC and the SPB/MTOCs; however, plant MOZRT1 is shown to directly bind to GCP3 (Janski *et al.*, 2008, 2012; Nakamura *et al.*, 2012). (B) In the absence of Mzt1 function (*mzt1* mutants), the core γ-TuC is still capable of assembling; however, this complex is unable to be recruited to the SPB/MTOCs. (C) In the absence of Alp6 function (*alp6-719* mutant), on the other hand, the core γ-TuC fails to be formed. Mzt1, on its own, is not sufficient to localize to the SPB/MTOCs; instead, all the four γ-TuC components (γ-tubulin/GCP1, Alp4/GCP2, Alp6/GCP3, and Mzt1/MOZART1) are required for complex recruitment to the SPB/MTOCs.

(Photometrics, Tucson, AZ) that was equipped with a temperature-controlled chamber (Precision Control, Seattle, WA). Live cells were imaged in a glass-bottom culture dish (MatTek Corporation, Ashland, MA) coated with soybean lectin at 27°C or at 36°C for temperature-sensitive mutants. The temperature-sensitive mutant cells were cultured in rich YE5S media until mid–log phase at 27°C and were subsequently shifted to the restrictive temperature of 36°C for further culture until observation.

For quantification of Mzt1 and Alp4 levels at the SPB and spindle microtubule levels, 12–14 sections were taken along the *z*-axis at 0.3-μm intervals. After deconvolution, projection images of maximum intensity were obtained, and maximum fluorescence intensities over the background intensity were used for statistical data analysis.

Immunochemical assays

Protein was extracted by mechanical shaking of cells in protein extraction buffer (50 mM HEPES, 50 mM NaF, 50 mM Na-β-glycerophosphate, 5 mM EGTA, 5 mM EDTA, 0.2% Triton X-100, with added 1× protease inhibitor cocktail [PIC; Sigma-Aldrich], 1 mM phenylmethylsulfonyl fluoride [PMSF]) with acid-washed glass beads in the FastPrep FP120 apparatus (4 × 30 s, power 6.0). Extracts were cleared of debris by centrifugation for 1 min and, subsequently, 5 min at 13,000 × *g*, and the concentration was determined by Bradford assay (Bio-Rad, Hercules, CA). A range of 3–10 mg of protein was used per pull-down experiment, in which the extract was incubated with slow rotation for 1 h, 30 min with GFP-Trap, GFP-binding protein coupled to magnetic particles (ChromoTek GmbH, Planegg-Martinsried, Germany). The beads were then washed in wash buffer (50 mM Tris-HCl, pH 7.4, 1 mM EDTA, 150 mM NaCl, 0.05% NP-40, 10% glycerol, 1 mM dithiothreitol, 1.5 mM *p*-nitrophenyl phosphate with added 1× PIC, 0.1 mM PMSF) and boiled in Laemmli buffer for 5 min. Protein extract was loaded and resolved on denaturing 4–12% gradient gels (Bio-Rad) and transferred by wet transfer onto polyvinylidene fluoride membrane. Membranes were blocked with 10% skim milk and blotted with either anti-GFP (Roche, Basel, Switzerland; and Torrey Pines Biolabs, Secaucus, NJ), anti-HA (Covance, Princeton, NJ), or affinity-purified rabbit anti–fission yeast γ-tubulin antibodies (Masuda and Shibata, 1996) at a dilution of 1:1000 in ImmunoShot solution 1 (Cosmo Bio, Tokyo, Japan). After washing, blots were incubated in anti-mouse horseradish peroxidase–conjugated secondary antibody (GE Healthcare, Buckinghamshire, UK) in ImmunoShot Solution 2 (Cosmo Bio) at a dilution of 1:2000. The ECL chemiluminescence kit (GE Healthcare) was used for detection.

ACKNOWLEDGMENTS

We thank Yuji Chikashige and Yasushi Hiraoka for providing us with vector plasmids and Takayuki Koyano, Kazunori Kume, and Dai Hirata for technical help for strain constructions. We are grateful to Tetsuya Horio, Berl Oakley, and Kayoko Tanaka for stimulating discussions and communication of unpublished results and to Dai Hirata and Eiko Tsuchiya for continuous encouragement. M.Y. was supported by the Strategic Young Researcher Overseas Visits Program for Accelerating Brain Circulation from the Japan Society for the Promotion of Science. This research was supported by Cancer Research UK (T.T.).

REFERENCES

Aldaz H, Rice LM, Stearns T, Agard DA (2005). Insights into microtubule nucleation from the crystal structure of human γ-tubulin. Nature 435, 523–527.

Anders A, Lourenco PC, Sawin KE (2006). Noncore components of the fission yeast γ-tubulin complex. Mol Biol Cell 17, 5057–5093.

Anders N, Sawin KE (2011). Microtubule stabilization in vivo by nucleation-incompetent γ-tubulin complex. J Cell Sci 124, 1207–1213.

Bähler J, Wu J, Longtine MS, Shah NG, McKenzie A, III, Steever AB, Wach A, Philippsen P, Pringle JR (1998). Heterologous modules for efficient and versatile PCR-based gene targeting in *Schizosaccharomyces pombe*. Yeast 14, 943–951.

Barr AR, Kilmartin JV, Gergely F (2010). CDK5RAP2 functions in centrosome to spindle pole attachment and DNA damage response. J Cell Biol 189, 23–39.
Bechhoefer J, Rhind N (2012). Replication timing and its emergence from stochastic processes. Trends Genet 28, 374–381.
Bitton DA, Wood V, Scutt PJ, Grallert A, Yates T, Smith DL, Hagan IM, Miller CJ (2011). Augmented annotation of the *Schizosaccharomyces pombe* genome reveals additional genes required for growth and viability. Genetics 187, 1207–1217.
Bouissou A, Verollet C, Sousa A, Sampaio P, Wright M, Sunkel CE, Merdes A, Raynaud-Messina B (2009). γ-Tubulin ring complexes regulate microtubule plus end dynamics. J Cell Biol 187, 327–334.
Boveri T (2008). Concerning the origin of malignant tumours by Theodor Boveri. Translated and annotated by H Harris. J Cell Sci 121, 1–84.
Bratman SV, Chang F (2007). Stabilization of overlapping microtubules by fission yeast CLASP. Dev Cell 13, 812–827.
Brinkley RR (1985). Microtubule organizing centers. Annu Rev Cell Biol 1, 145–172.
Chang L, Gould KL (2000). Sid4p is required to localize components of the septation initiation pathway to the spindle pole body in fission yeast. Proc Natl Acad Sci USA 97, 5249–5254.
Choi YK, Liu P, Sze SK, Dai C, Qi RZ (2010). CDK5RAP2 stimulates microtubule nucleation by the γ-tubulin ring complex. J Cell Biol 191, 1089–1095.
Desai A, Mitchison TJ (1997). Microtubule polymerization dynamics. Annu Rev Cell Dev Biol 13, 83–117.
Drummond DR, Cross RA (2000). Dynamics of interphase microtubules in *Schizosaccharomyces pombe*. Curr Biol 10, 766–775.
Ehrhardt DW, Shaw SL (2006). Microtubule dynamics and organization in the plant cortical array. Annu Rev Plant Biol 57, 859–875.
Fava F, Raynaud-Messina B, Leung-Tack J, Mazzolini L, Li M, Guillemot JC, Cachot D, Tollon Y, Ferrara P, Wright M (1999). Human 76p: a new member of the γ-tubulin–associated protein family. J Cell Biol 147, 857–868.
Fong CS, Sato M, Toda T (2010). Fission yeast Pcp1 links polo kinase-mediated mitotic entry to γ-tubulin-dependent spindle formation. EMBO J 29, 120–130.
Fong KW, Choi YK, Rattner JB, Qi RZ (2008). CDK5RAP2 is a pericentriolar protein that functions in centrosomal attachment of the γ-tubulin ring complex. Mol Biol Cell 19, 115–125.
Fujita A, Vardy L, Garcia MA, Toda T (2002). A fourth component of the fission yeast γ-tubulin complex, Alp16, is required for cytoplasmic microtubule integrity and becomes indispensable when γ-tubulin function is compromised. Mol Biol Cell 13, 2360–2373.
Geissler S, Pereira G, Spang A, Knop M, Souès S, Kilmartin J, Schiebel E (1996). The spindle pole body component Spc98p interacts with the γ-tubulin-like Tub4p of *Saccharomyces cerevisiae* at the sites of microtubule attachment. EMBO J 15, 3899–3911.
Guillet V *et al.* (2011). Crystal structure of γ-tubulin complex protein GCP4 provides insight into microtubule nucleation. Nat Struct Mol Biol 18, 915–919.
Gunawardane RN, Lizarraga SB, Wiese C, Wilde A, Zheng Y (2000a). γ-Tubulin complexes and their role in microtubule nucleation. Curr Top Dev Biol 49, 55–73.
Gunawardane RN, Martin OC, Cao K, Zhang L, Dej K, Iwamatsu A, Zheng Y (2000b). Characterization and reconstitution of *Drosophila* γ-tubulin ring complex subunits. J Cell Biol 151, 1513–1524.
Gunawardane RN, Martin OC, Zheng Y (2003). Characterization of a new γTuRC subunit with WD repeats. Mol Biol Cell 14, 1017–1026.
Hagan IM, Petersen J (2000). The microtubule organizing centers of *Schizosaccharomyces pombe*. Curr Top Dev Biol 49, 133–159.
Haren L, Remy MH, Bazin I, Callebaut I, Wright M, Merdes A (2006). NEDD1-dependent recruitment of the γ-tubulin ring complex to the centrosome is necessary for centriole duplication and spindle assembly. J Cell Biol 172, 505–515.
Hauf S, Biswas A, Langegger M, Kawashima SA, Tsukahara T, Watanabe Y (2007). Aurora controls sister kinetochore mono-orientation and homolog bi-orientation in meiosis-I. EMBO J 26, 4475–4486.
Hendrickson TW, Yao J, Bhadury S, Corbett AH, Joshi HC (2001). Conditional mutations in γ-tubulin reveal its involvement in chromosome segregation and cytokinesis. Mol Biol Cell 12, 2469–2481.
Hoog JL, Schwartz C, Noon AT, O'Toole ET, Mastronarde DN, McIntosh JR, Antony C (2007). Organization of interphase microtubules in fission yeast analyzed by electron tomography. Dev Cell 12, 349–361.
Horio T, Oakley BR (1994). Human γ-tubulin functions in fission yeast. J Cell Biol 126, 1465–1473.
Horio T, Uzawa S, Jung MK, Oakley BR, Tanaka K, Yanagida M (1991). The fission yeast γ-tubulin is essential for mitosis and is localized at microtubule organizing centers. J Cell Sci 99, 693–700.
Hsu KS, Toda T (2011). Ndc80 internal loop interacts with Dis1/TOG to ensure proper kinetochore-spindle attachment in fission yeast. Curr Biol 21, 214–220.
Hutchins JR *et al.* (2010). Systematic analysis of human protein complexes identifies chromosome segregation proteins. Science 328, 593–599.
Janski N, Herzog E, Schmit AC (2008). Identification of a novel small *Arabidopsis* protein interacting with γ-tubulin complex protein 3. Cell Biol Int 32, 546–548.
Janski N, Masoud K, Batzenschlager M, Herzog E, Evrard JL, Houlne G, Bourge M, Chaboute ME, Schmit AC (2012). The GCP3-interacting proteins GIP1 and GIP2 are required for γ-tubulin complex protein localization, spindle integrity, and chromosomal stability. Plant Cell 24, 1171–1187.
Janson ME, Setty TG, Paoletti A, Tran PT (2005). Efficient formation of bipolar microtubule bundles requires microtubule-bound γ-tubulin complexes. J Cell Biol 169, 297–308.
Jiang K, Akhmanova A (2011). Microtubule tip-interacting proteins: a view from both ends. Curr Opin Cell Biol 23, 94–101.
Job D, Valiron O, Oakley B (2003). Microtubule nucleation. Curr Opin Cell Biol 15, 111–117.
Joshi HC, Palacios MJ, McNamara L, Cleveland DW (1992). γ-Tubulin is a centrosomal protein required for cell cycle-dependent microtubule nucleation. Nature 356, 80–83.
Knop M, Pereira G, Geissler S, Grein K, Schiebel E (1997). The spindle pole body component Spc97p interacts with the γ-tubulin of *Saccharomyces cerevisiae* and functions in microtubule organization and spindle pole body duplication. EMBO J 16, 1550–1564.
Kollman JM, Merdes A, Mourey L, Agard DA (2011). Microtubule nucleation by γ-tubulin complexes. Nat Rev Mol Cell Biol 12, 709–721.
Kollman JM, Polka JK, Zelter A, Davis TN, Agard DA (2010). Microtubule nucleating γ-TuSC assembles structures with 13-fold microtubule-like symmetry. Nature 466, 879–882.
Li S, Fernandez JJ, Marshall WF, Agard DA (2012). Three-dimensional structure of basal body triplet revealed by electron cryo-tomography. EMBO J 31, 552–562.
Luders J, Patel UK, Stearns T (2006). GCP-WD is a γ-tubulin targeting factor required for centrosomal and chromatin-mediated microtubule nucleation. Nat Cell Biol 8, 137–147.
Luders J, Stearns T (2007). Microtubule-organizing centres: a re-evaluation. Nat Rev Mol Cell Biol 8, 161–167.
Marschall LG, Jeng RL, Mulholland J, Stearns T (1996). Analysis of Tub4p, yeast γ-tubulin-like protein: implications for microtubule-organizing center function. J Cell Biol 134, 443–454.
Martin OC, Gunawardane RN, Iwamatsu A, Zheng Y (1998). Xgrip109: a γ tubulin-associated protein with an essential role in γ-tubulin ring complex (γTuRC) assembly and centrosome function. J Cell Biol 141, 675–687.
Masuda H, Miyamoto R, Haraguchi T, Hiraoka Y (2006a). The carboxy-terminus of Alp4 alters microtubule dynamics to induce oscillatory nuclear movement led by the spindle pole body in *Schizosaccharomyces pombe*. Genes Cells 11, 337–352.
Masuda H, Sevik M, Cande WZ (1992). In vitro microtubule-nucleating activity of spindle pole bodies in fission yeast *Schizosaccharomyces pombe*: cell cycle-dependent activation in *Xenopus* cell-free extracts. J Cell Biol 117, 1055–1066.
Masuda H, Shibata T (1996). Role of γ-tubulin in mitosis-specific microtubule nucleation from the *Schizosaccharomyces pombe* spindle pole body. J Cell Sci 109, 165–177.
Masuda H, Toda T, Miyamoto R, Haraguchi T, Hiraoka Y (2006b). Modulation of Alp4 function in *Schizosaccharomyces pombe* induces novel phenotypes that imply distinct functions for nuclear and cytoplasmic γ-tubulin complexes. Genes Cells 11, 319–336.
Meng W, Mushika Y, Ichii T, Takeichi M (2008). Anchorage of microtubule minus ends to adherens junctions regulates epithelial cell-cell contacts. Cell 135, 948–959.
Mishra RK, Chakraborty P, Arnaoutov A, Fontoura BM, Dasso M (2010). The Nup107–160 complex and γ-TuRC regulate microtubule polymerization at kinetochores. Nat Cell Biol 12, 164–169.
Moreno S, Klar A, Nurse P (1991). Molecular genetic analyses of fission yeast *Schizosaccharomyces pombe*. Methods Enzymol 194, 773–782.
Moritz M, Agard DA (2001). γ-Tubulin complexes and microtubule nucleation. Curr Opin Struct Biol 11, 174–181.

Moritz M, Braufeld MB, Dedat JW, Alberts B, Agard DA (1995). Microtubule nucleation by γ-tubulin-containing rings in the centrosome. Nature 378, 638–640.
Moritz M, Zheng Y, Alberts BM, Oegema K (1998). Recruitment of the γ-tubulin ring complex to *Drosophila* salt-stripped centrosome scaffolds. J Cell Biol 142, 775–786.
Murata T, Sonobe S, Baskin TI, Hyodo S, Hasezawa S, Nagata T, Horio T, Hasebe M (2005). Microtubule-dependent microtubule nucleation based on recruitment of γ-tubulin in higher plants. Nat Cell Biol 7, 961–968.
Murphy SM, Urbani L, Stearns T (1998). The mammalian γ-tubulin complex contains homologues of the yeast spindle pole body components Spc97p and Spc98p. J Cell Biol 141, 663–674.
Nakamura M, Yagi N, Kato T, Fujita S, Kawashima N, Ehrhardt DW, Hashimoto T (2012). *Arabidopsis* GCP3-interacting protein 1/MOZART1 is an integral component of the γ-tubulin-containing microtubule nucleating complex. Plant J 71, 216–225.
Nogales E (2000). Structural insights into microtubule function. Annu Rev Biochem 69, 277–302.
Oakley BR, Oakley CE, Yoon Y, Jung MK (1990). γ-Tubulin is a component of the spindle pole body that is essential for microtubule function in *Aspergillus nidulans*. Cell 61, 1289–1301.
Oakley CE, Oakley BR (1989). Identification of γ-tubulin, a new member of the tubulin superfamily encoded by *mipA* gene of *Aspergillus nidulans*. Nature 338, 662–664.
Oegema K, Wiese C, Martin OC, Milligan RA, Iwamatsu A, Mitchison TJ, Zheng Y (1999). Characterization of two related *Drosophila* γ-tubulin complexes that differ in their ability to nucleate microtubules. J Cell Biol 144, 721–733.
Paluh JL, Nogales E, Oakley BR, McDonald K, Pidoux AL, Cande WZ (2000). A mutation in γ-tubulin alters microtubule dynamics and organization and is synthetically lethal with the kinesin-like protein Pkl1p. Mol Biol Cell 11, 1225–1239.
Pickett-Heaps JD (1969). The evolution of the mitotic apparatus: an attempt at comparative ultrastructural cytology in dividing plant cells. Cytobios 3, 257–280.
Pinyol R, Scrofani J, Vernos I (2013). The role of NEDD1 phosphorylation by Aurora A in chromosomal microtubule nucleation and spindle function. Curr Biol 23, 143–149.
Samejima I, Miller VJ, Groocock LM, Sawin KE (2008). Two distinct regions of Mto1 are required for normal microtubule nucleation and efficient association with the γ-tubulin complex in vivo. J Cell Sci 121, 3971–3980.
Sato M, Dhut S, Toda T (2005). New drug-resistant cassettes for gene disruption and epitope tagging in *Schizosaccharomyces pombe*. Yeast 22, 583–591.
Sawin KE, Lourenco PCC, Snaith HA (2004). Microtubule nucleation at non-spindle pole body microtubule-organizing centers requires fission yeast centrosomin-related protein mod20p. Curr Biol 14, 763–775.
Sawin KE, Tran PT (2006). Cytoplasmic microtubule organization in fission yeast. Yeast 23, 1001–1014.
Sobel SG, Snyder M (1995). A highly divergent γ-tubulin gene is essential for cell growth and proper microtubule organization in *Saccharomyces cerevisiae*. J Cell Biol 131, 1775–1788.
Spang A, Geissler S, Grein K, Schiebel E (1996). γ-Tubulin-like Tub4p of *Saccharomyces cerevisiae* is associated with the spindle pole body substructures that organize microtubules and is required for mitotic spindle formation. J Cell Biol 134, 429–441.
Stearns T, Evans L, Kirschner M (1991). γ-Tubulin is a highly conserved component of the centrosome. Cell 65, 825–836.
Stearns T, Kirschner M (1994). In vitro reconstitution of centrosome assembly and function: the central role of γ-tubulin. Cell 76, 623–637.
Takahashi M, Yamagiwa A, Nishimura T, Mukai H, Ono Y (2002). Centrosomal proteins CG-NAP and kendrin provide microtubule nucleation sites by anchoring γ-tubulin ring complex. Mol Biol Cell 13, 3235–3245.
Tanaka N, Meng W, Nagae S, Takeichi M (2012). Nezha/CAMSAP3 and CAMSAP2 cooperate in epithelial-specific organization of noncentrosomal microtubules. Proc Natl Acad Sci USA 109, 20029–20034.
Tange Y, Fujita A, Toda T, Niwa N (2004). Functional dissection of the γ-tubulin complex by suppressor analysis of *gtb1* of *alp4* mutations in *Schizosaccharomyces pombe*. Genetics 167, 1095–1107.
Tassin A-M, Celati C, Moudjou M, Bornens M (1998). Characterization of the human homologue of the yeast Spc98p and its association with γ-tubulin. J Cell Biol 141, 689–701.
Teixido-Travesa N, Roig J, Luders J (2012). The where, when and how of microtubule nucleation—one ring to rule them all. J Cell Sci 125, 4445–4456.
Teixido-Travesa N, Villen J, Lacasa C, Bertran MT, Archinti M, Gygi SP, Caelles C, Roig J, Luders J (2010). The γTuRC revisited: a comparative analysis of interphase and mitotic human γTuRC redefines the set of core components and identifies the novel subunit GCP8. Mol Biol Cell 21, 3963–3972.
Toda T, Adachi Y, Hiraoka Y, Yanagida M (1984). Identification of the pleiotropic cell division cycle gene *NDA2* as one of two different α-tubulin genes in *Schizosaccharomyces pombe*. Cell 37, 233–242.
Tran PT, Marsh L, Doye V, Inoue S, Chang F (2001). A mechanism for nuclear positioning in fission yeast based on microtubule pushing. J Cell Biol 153, 397–412.
Vardy L, Fujita A, Toda T (2002). The γ-tubulin complex protein Alp4 provides a link between the metaphase checkpoint and cytokinesis in fission yeast. Genes Cells 7, 365–373.
Vardy L, Toda T (2000). The fission yeast γ-tubulin complex is required in G_1 phase and is a component of the spindle assembly checkpoint. EMBO J 19, 6098–6111.
Venkatram S, Tasto JJ, Feoktistova A, Jennings JL, Link AJ, Gould KL (2004). Identification and characterization of two novel proteins affecting fission yeast γ-tubulin complex function. Mol Biol Cell 15, 2287–2301.
Verollet C, Colombie N, Daubon T, Bourbon HM, Wright M, Raynaud-Messina B (2006). *Drosophila melanogaster* γ-TuRC is dispensable for targeting γ-tubulin to the centrosome and microtubule nucleation. J Cell Biol 172, 517–528.
Vinh DBN, Kern JW, Hancock WO, Howard J, Davis TN (2002). Reconstitution and characterization of budding yeast γ-tubulin complex. Mol Biol Cell 13, 1144–1157.
Wiese C, Zheng Y (2006). Microtubule nucleation: γ-tubulin and beyond. J Cell Sci 119, 4143–4153.
Xiong Y, Oakley BR (2009). In vivo analysis of the functions of γ-tubulin-complex proteins. J Cell Sci 122, 4218–4227.
Zhang J, Megraw TL (2007). Proper recruitment of γ-tubulin and D-TACC/Msps to embryonic *Drosophila* centrosomes requires centrosomin motif 1. Mol Biol Cell 10, 4037–4049.
Zhang L, Keating TJ, Wilde A, Borisy GG, Zheng Y (2000). The role of Xgrip210 in γ-tubulin ring complex assembly and centrosome recruitment. J Cell Biol 151, 1525–1536.
Zheng Y, Jung MK, Oakley BR (1991). γ-Tubulin is present in *Drosophila melanogaster* and *Homo sapiens* and is associated with the centrosome. Cell 65, 817–823.
Zheng Y, Wong ML, Alberts B, Mitchison T (1995). Nucleation of microtubule assembly by a γ-tubulin-containing ring complex. Nature 378, 578–583.
Zimmerman S, Chang F (2005). Effects of γ-tubulin complex proteins on microtubule nucleation and catastrophe in fission yeast. Mol Biol Cell 16, 2719–2733.
Zimmerman WC, Sillibourne J, Rosa J, Doxsey SJ (2004). Mitosis-specific anchoring of γ-tubulin complexes by pericentrin controls spindle organization and mitotic entry. Mol Biol Cell 15, 3642–3657.